Extracellular Vesicles and Particles Modulate Proton Secretion in a Model of Human Parietal Cells

Agnes Mistlberger-Reiner,* Sonja Sterneder, Siegfried Reipert, Sara Wolske, and Veronika Somoza

Read Online

ACCESS | Metrics & More | Article Recommendations | Supporting Information

ABSTRACT: The secretion of extracellular vesicles and particles (EVPs) is an important mechanism of cellular communication. In this work, we demonstrate a functional role of EVPs in mechanisms regulating gastric acid secretion. HGT-1 cells were used as a model system to assess proton secretion. First, in order to prove EVP secretion by HGT-1 cells, EVPs were isolated by size exclusion chromatography and characterized by nanoparticle tracking analysis, Western blot, and cryo transmission electron microscopy. For examination of the potential role of EVPs in proton secretion, HGT-1 cells were treated with pharmacological EV-inhibitors, resulting in a reduction of histamine-induced proton secretion. To demonstrate the functional role of EVPs in the mechanism of proton secretion, EVP-conditioned supernatant was collected after stimulation of HGT-1 cells with histamine, fractionated, and subjected to an activity screening. The results revealed constituents of the HGT-1-derived secretome with an MW of >100 kDa (including EVPs) to modulate proton secretion, while smaller constituents had no effect. Finally, a dose-dependent modulatory effect on proton secretion of HGT-1 cells was demonstrated by isolated HGT-1-derived EVPs. Hence, this study presents first results on the potential function of EVPs as a previously undiscovered mechanism of regulation of gastric acid secretion by parietal cells.
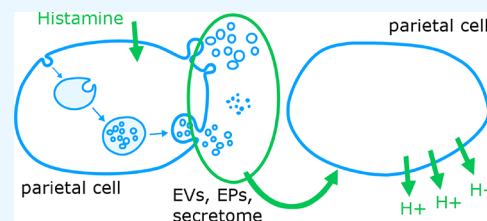
INTRODUCTION

In the early 1980s, a new class of cellular secretory vesicles was first described.[1,2] In the beginning believed to be waste disposal systems of cells, we now know that extracellular vesicles (EVs) participate in intercellular communication and are involved in many physiological and pathological processes in cells and tissues. Exosomes and microvesicles (MVs) are the two main classes of EVs. The former are built by inward budding of the endosomal membrane and fusion of such multivesicular bodies (MVBs) with the plasma membrane.[3] The later are formed through direct outward budding at the plasma membrane.[3] Besides EVs, extracellular particles (EPs), including, for example, exomeres, supermeres, or lipoproteins, are also secreted by cells and are involved in functional roles of the cellular secretome.[4−6] Since EVs and EPs are often coisolated and difficult to discriminate with current analysis techniques, due to their overlapping physical or chemical properties, in this study, the term EVPs is used whenever the coexistence of EVs and EPs cannot be excluded.

Even though the potential role of EVPs in diverse physiological functions has already been the topic of several studies, summarized by Yáñez-Mó et al.,[7] most studies focused on functions in diseased states because EVPs hold potential as novel disease biomarkers and in disease therapy, as reviewed by Kalluri and LeBleu.[8] The same is true for studies on EVPs derived from gastric cells and tissues. While much effort was put into the study of the relevance and functions of EVPs in carcinogenesis, metastatic processes and therapy of gastric cancer, as reviewed in refs 9−11, knowledge of the gastric

functions of EVPs is scarce. In one study, EVPs were identified in gastric juice of gastric cancer patients and reported to increase the viability of human skin fibroblasts in culture.[12] These results suggest an active modification of the cancer cells' microenvironment by gastric juice-derived EVPs. We, therefore, hypothesize that gastric EVPs functionally modify distinct mechanisms of gastric cells.

The primary mechanism of gastric cells is the secretion of gastric acid, which is necessary for the digestion of dietary proteins. Nevertheless, this acid secretion is tightly regulated by a complex network of agonists and antagonists in order to protect gastric tissues from damage from the acidic environment.[13] This neuroendocrine regulatory system includes the direct activation of parietal cells by histamine binding to histamine H2 receptors[14] and the hormone gastrin binding to cholecystokinin B receptors.[15,16] Additionally, gastrin activates enterochromaffin-like cells to release histamine,[17] which again stimulates parietal cells, thus indirectly activating gastric acid secretion. The hormone ghrelin activates parietal cells indirectly via the enteric nervous system,[13] which transfers signals from the vagus nerve via acetylcholine by binding to
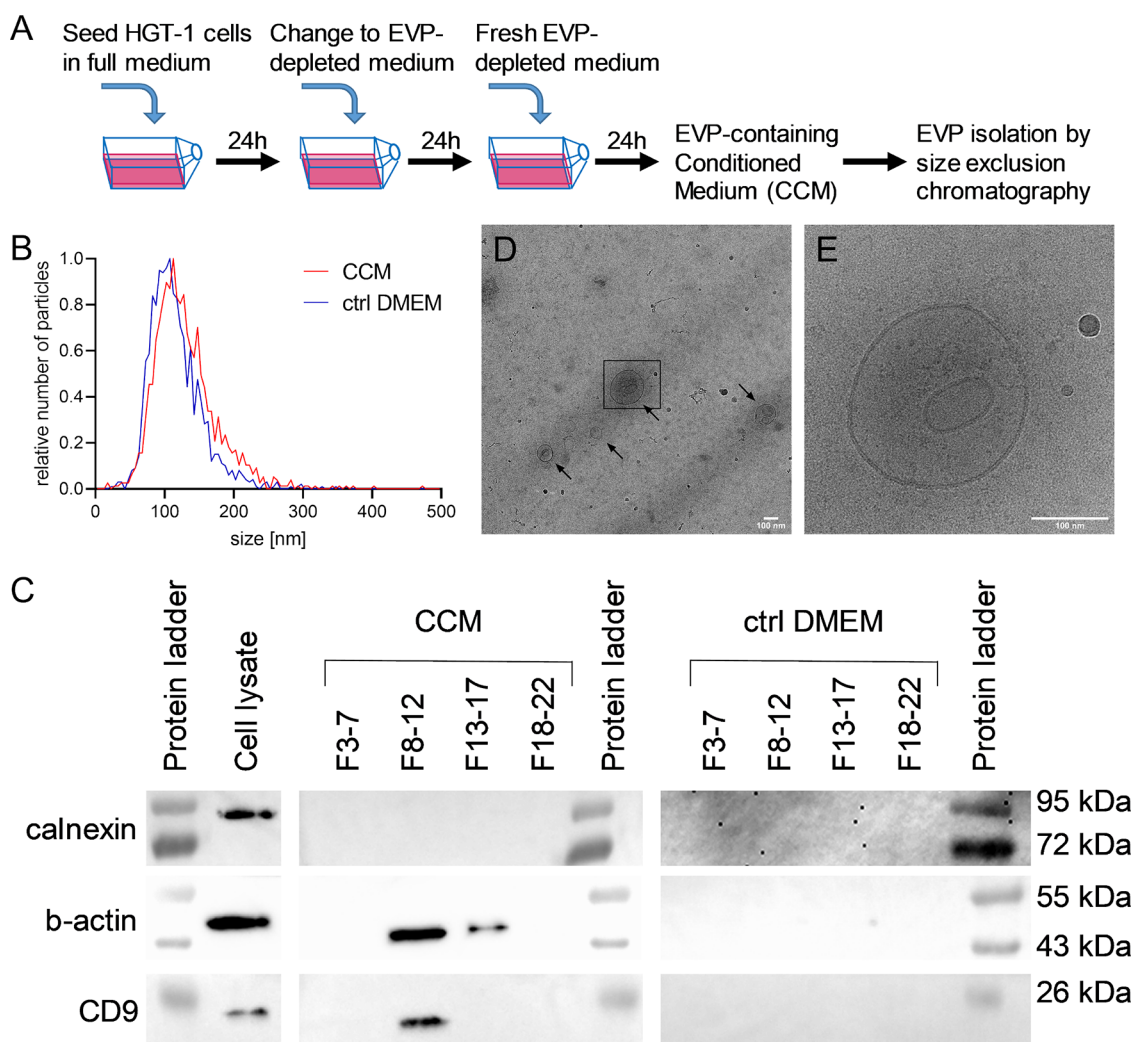
Figure 1. Characterization of HGT-1-derived EVPs. (A) Schematic illustration of EVP-conditioning and isolation protocol for HGT-1 EVP characterization. (B) Exemplary size distribution of EVPs isolated from cell culture medium conditioned by HGT-1 cells for 24 h (CCM) and from unconditioned cell culture medium (ctrl DMEM) measured with nanoparticle tracking analysis. (C) Western blot analysis of EVP-protein markers b-actin and CD9 and non-EVP protein marker Calnexin in HGT-1 cell lysate and pooled and concentrated fractions collected from size exclusion chromatography of CCM or ctrl DMEM (for images of the whole membranes, see Figure S4). (D, E) Cryo transmission electron microscopy image of several isolated EVPs indicated by arrows (D, scale bar = 100 nm) and close-up of two EVs shown in the black square in Figure 1D (E, scale bar = 100 nm).

muscarinic acetylcholine receptor M3 on parietal cells.[18] One of the most important endogenous inhibitors of gastric acid secretion is the hormone somatostatin, which inactivates parietal cells directly through binding to somatostatin receptors.[19,20] In addition to these well-established routes, other molecules, like bitter taste receptor agonists and antagonists, were also shown to modulate gastric acid secretion.[21] The stimulation of parietal cells through receptor-specific agonists results in the activation of signal transduction pathways involving an increase in cyclic AMP levels for histamine activation[22,23] and activation of bitter taste receptor TAS2R43[21] or an increase in intracellular Ca^{2+}-levels and protein kinase C activation for muscarinic acetylcholine receptor M3 activation.[24,25] Finally, cellular reorganization leads to the transfer of the proton pump H^+-K^+-ATPase from intracellular tubulovesicles to the cell surface, where the enzyme starts to pump protons into the gastric lumen.[26,27]

Notably, G-protein coupled receptors similar to those described for regulation of gastric acid secretion were also reported to modulate EVP secretion. In more detail, an increase in EV or EVP secretion was shown after agonist stimulation of the muscarinic acetylcholine receptor M1 and M3 in T-lymphocytes[28] and trophoblast cells,[29] the cholecystokinin B receptor and the bitter taste receptor TAS2R14 also in trophoblast cells,[29] and the histamine H1 receptor in HeLa and HUVEC cells.[30] Consequently, EVPs might also play a yet unknown role in mechanisms regulating gastric acid secretion.

The human gastric cell line HGT-1 is an established model system to analyze the regulation of gastric acid secretion by measuring the amount of protons secreted by the cells upon stimulation.[21,31−39] As already shown in earlier studies,[21,37,38] this model system closely resembles physiological conditions, since effects of agonists and antagonists on proton secretion of HGT-1 cells correlate with pH-measurements taken directly in the human stomach using Heidelberg capsules. Hence, HGT-1 cells and their mechanism of proton secretion as functional
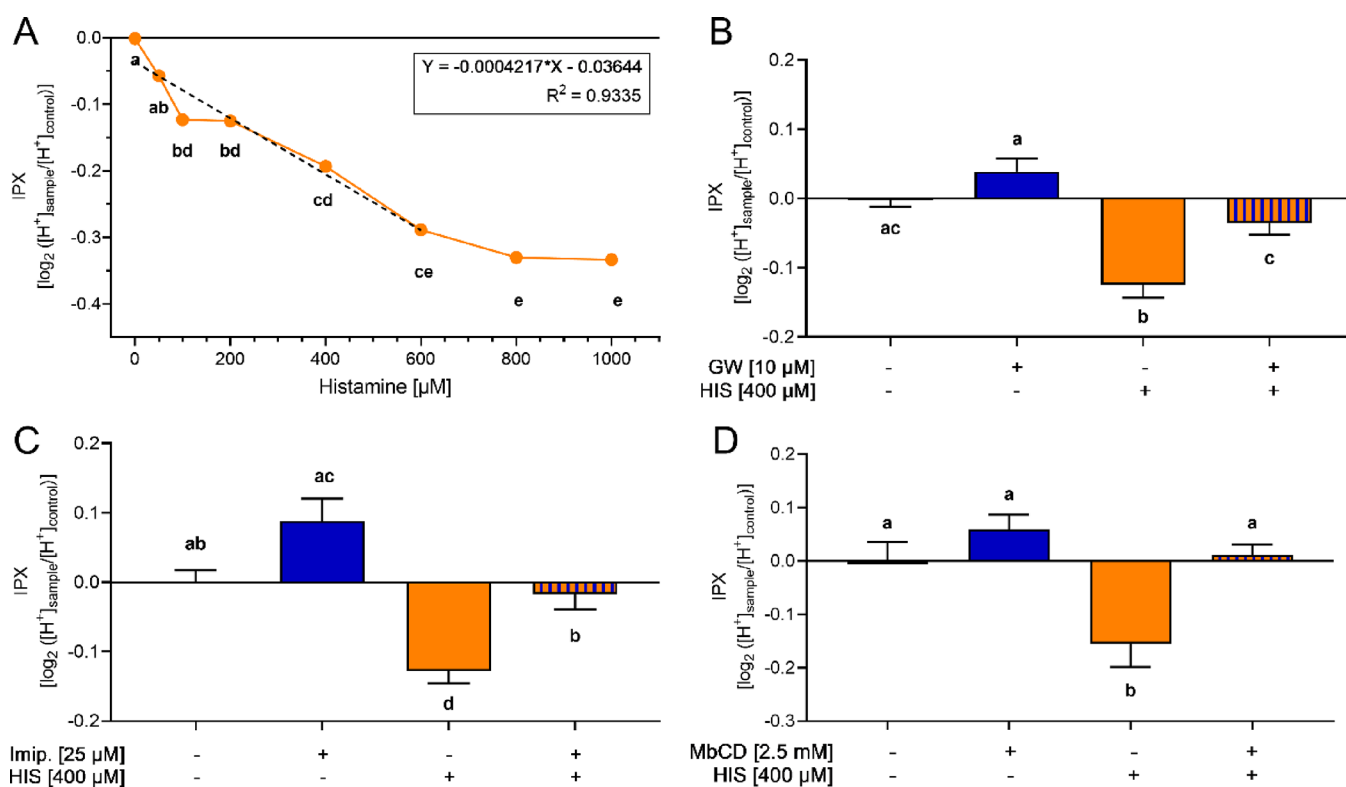
Figure 2. Effects of EVP inhibition on proton secretion. Intracellular proton index (IPX) of HGT-1 cells treated with (A) indicated concentrations of histamine (HIS) for 10 min w/o (B) pre-incubation with GW4869 (GW) for 24 h, (C) pre-incubation with Imipramine (Imip.) for 60 min, and (D) pre-incubation with methyl-β-cyclodextrin (MbCD) for 15 min, compared to control cells. Data are shown as mean $\pm$ SEM, $n = 3-4$, t.r. $=3-6$. Statistics: one-way ANOVA on ranks followed by post hoc Holm−Sidak test (A, B, D) and Dunn's method (C). Different letters indicate significant differences at a level of $p < 0.05$.

outcome were used in this study to explore the role of EVPs in gastric acid secretion.

RESULTS

Characterization of HGT-1 Cell-Derived EVPs. In order to demonstrate that HGT-1 cells secrete EVPs, HGT-1 cells were cultivated for 24 h in EVP-depleted cell culture medium to produce EVP-conditioned cell culture medium (CCM), as illustrated in Figure 1A. By isolation and consecutive analysis of EVPs from the CCM, it could be proven that HGT-1 cells secrete EVPs and that the procedure of the isolation protocol yielded EVPs. As control, the same isolation protocol and analysis was performed with EVP-unconditioned medium (ctrl DMEM), which was never in contact with cells. Different fractions separated by size exclusion chromatography were collected and analyzed by nanoparticle tracking analysis, Bradford analysis, Western blot, and ELISA. Cryo transmission electron microscopy (cryo TEM) of the EVP-containing fraction was performed to show the vesicular nature of the isolated particles.

First, different fractions were collected after size exclusion chromatography resembling the void volume (F3−7), the EVP fraction (F8−12), an intermediate size fraction (F13−17), and the protein fraction (F18−22). As hypothesized, the comparison of the particle and the protein concentration in each of these fractions proved the separation of EVPs from protein, with F8−12 containing most of EVPs and very low protein levels and F18−22 containing high protein levels and low EVP concentrations (see Figure S1). Hence, F8−12 was

used for further analysis and characterization of HGT-1-derived EVPs.

A total of $4.8 \pm 1.5 \times 10^{10}$ particles was isolated from CCM conditioned by $2.3 \pm 1.1 \times 10^7$ cells with a mean viability of $93.5 \pm 2.9\%$, while $2.6 \pm 1.8 \times 10^{10}$ particles were measured in F8−12 from the same volume of unconditioned, EVP-depleted medium, which corresponds to about half of the isolated particles from the CCM. An exemplary size distribution of the particles, analyzed by nanoparticle tracking analysis, is shown in Figure 1B. EVPs isolated from CCM had a larger median size of 118.3 ± 1.1 nm compared to those from ctrl DMEM with 109.5 ± 2.4 nm (two-tailed Student's t-test, p-value = 0.005). The zeta potential of these particles was -22.7 ± 5.4 and -16.9 ± 2.9 mV (two-tailed Student's t-test, p-value = 0.198). All given data are given as the mean and standard deviation of three biological replicates. In Figure 1C, images of the Western blot analysis for the proteins calnexin, β-actin, and CD9 in the different isolated fractions, as well as HGT-1 cell lysate are shown (images of the whole Western blot membranes are shown in Figure S4). β-actin and CD9 were used as EVP markers[40] and could be detected in the EVP-fraction (F8−12) from CCM, but not in the EVP-fraction isolated from ctrl DMEM. Therefore, the particles isolated from the unconditioned medium and measured by NTA might not be EVPs or might be below the detection limit, supporting the successful serum-derived EVP-depletion or at least reduction from the cell culture medium. As expected, calnexin was detected in the cell lysate but not in any of the fractions, since it is a protein of the endoplasmic reticulum that is present in cells but not in EVPs,[40] which supports that EVPs were
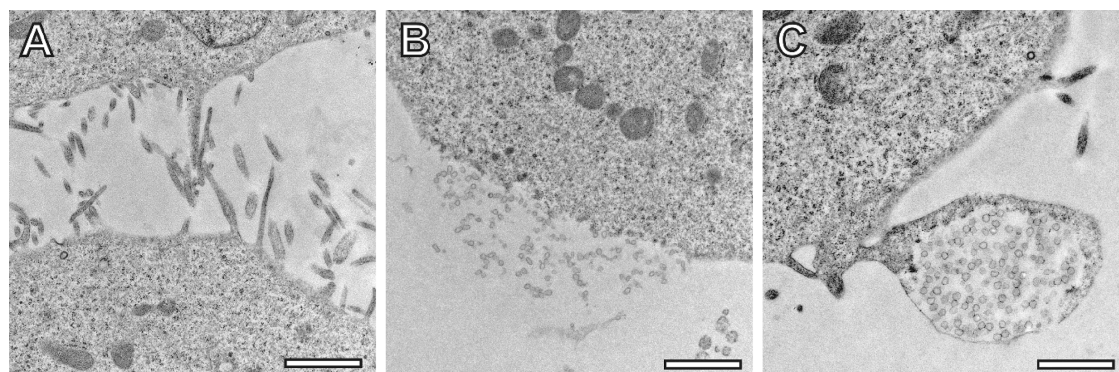
Figure 3. Examples of TEM-images of membranous structures of HGT-1 cells. (A) Detail of two neighboring HGT-1 cells both endowed with microvilli. (B) Local region of the plasma membrane showing a lipid membrane domain from which EVPs are secreted. It differs in its morphology from flat regions of the plasma membranes displayed in (A) and (B). (C) Big vesicle with multivesicular content attached to an HGT-1 cell surface (additional images in Figure S3). Images are examples and chosen from any images of HGT-1 cells taken after one of the four treatments (control, GW4869 pretreatment only, histamine stimulation only, GW4869 pretreatment and histamine stimulation) for the best image quality and visibility of the described structures because the treatments showed no effects on the cellular structures. Scale bars = 500 nm.

separated successfully from other cellular components by this isolation protocol. H^+-K^+-ATPase (α-subunit) was analyzed by ELISA as a cell type specific protein, which is crucial for the proton secretion activity of the cells,[27] and was only detectable in the cell lysate at a concentration of 15.0 ± 0.4 ng/mL but not in EVPs or other fractions.

The cryo TEM images of the EVP fraction F8−12 in Figure 1D,E display an overview of several HGT-1-derived particles, within the size range determined by nanoparticle tracking analysis, and a close-up of one particle that proves the presence of a lipid bilayer and, therefore, the vesicular nature of these particles. Since cryo TEM of the EVP-containing fraction showed mostly particles surrounded by a lipid bilayer, i.e., vesicles, it is suggested that most of the isolated particles are actually EVs. However, it cannot be excluded that EPs are also present by the methods used in this study.

EVP Inhibition Decreases Proton Secretion. To examine the role that EVPs might play in mechanisms regulating proton secretion, HGT-1 cells were treated with different substances known to inhibit the secretion of EVPs: (i) GW4869, which inhibits the enzyme neutral sphingomyelinase, thereby blocking the inward budding of exosomes into MVBs and their secretion;[30,41] (ii) imipramine hydrochloride as inhibitor of the acid sphingomyelinase, which is active at the plasma membrane and responsible for MV blebbing;[42,43] and (iii) methyl-β-cyclodextrin (MβCD), which removes cholesterol from the plasma membrane and therefore also inhibits MV formation.[44]

Since histamine was formerly used at a concentration of 1 mM in the proton secretion assay,[45,46] HGT-1 cells were stimulated with 1 mM histamine for 10 min after a 24 h pre-incubation with GW4869 in an initial set of experiments. The results showed no significant effect after GW4869 treatment (see Figure S2). However, stimulation of HGT-1 cells with a range of concentrations of histamine from 50 μM to 1 mM showed that saturation of the assay signal is reached when using 1 mM histamine, as illustrated in Figure 2A. Hence, it might not be possible to observe modulating effects by pre-incubations with the used inhibitor at this histamine concentration. Therefore, the assay with GW4869 treatment was repeated with a subsequent stimulation with 400 μM histamine, which was identified as the highest concentration before reaching histamine-induced signal saturation yet within

the linear range of cell response. As shown in Figure 2B, a significant decrease in proton secretion by $71.6 \pm 13.4\%$ (given as mean $\pm$ SEM, 100% equals to an IPX of -0.13 ± 0.02 achieved in non-inhibitor-treated cells, $p < 0.01$) by GW4869 compared to histamine stimulation without GW4869 pre-incubation was measured. Similar effects were detected when HGT-1 cells were treated with imipramine hydrochloride and MβCD prior to histamine stimulation, with a reduction of proton secretion by $86.3 \pm 17.0\%$ (given as mean $\pm$ SEM, 100% equals to an IPX of -0.13 ± 0.02 achieved in non-inhibitor-treated cells, $p < 0.05$) and $107.3 \pm 12.5\%$ (given as mean $\pm$ SEM, 100% equals to an IPX of -0.15 ± 0.04, $p < 0.05$), respectively (see Figure 2C,D). Notably, no statistically significant effects on proton secretion were measured, when the pre-incubated cells were analyzed without further histamine stimulation. Furthermore, cell viability of HGT-1 cells was not affected by the different treatments, as measured by the MTT assay (data not shown).

Since all three inhibitors used are known to inhibit EVP secretion[41−44] and led to a decreased proton secretion upon stimulation with histamine, the authors hypothesized that EVPs might play an activating role in the process of histamine-stimulated proton secretion.

Effects on Cellular Membrane Structures. GW4869, imipramine hydrochloride, and MβCD all act on the composition of cellular membranes and change their capability of producing vesicular structures. The process of gastric acid secretion by parietal cells *in vivo* also involves reorganization of cellular membranes, namely, the transfer of intracellular tubulovesicles to the plasma membrane and their fusion to form microvilli and increase the cell's surface area.[26,27] Consequently, we hypothesized the effects of the inhibitors on proton secretion to be associated with changes in cellular membrane structures and examined such potential changes caused by EVP inhibition and histamine stimulation by imaging of HGT-1 cells with TEM.

The inhibitory effect of imipramine hydrochloride and MβCD on EVP secretion has so far only been shown by indirect methods of EVP isolation and quantification of fluorescence signals by fluorescence microscopy[42] and flow cytometry,[43] or only by flow cytometry,[44] respectively. However, besides the verification by indirect measurements analyzing EVP protein content using Western blotting
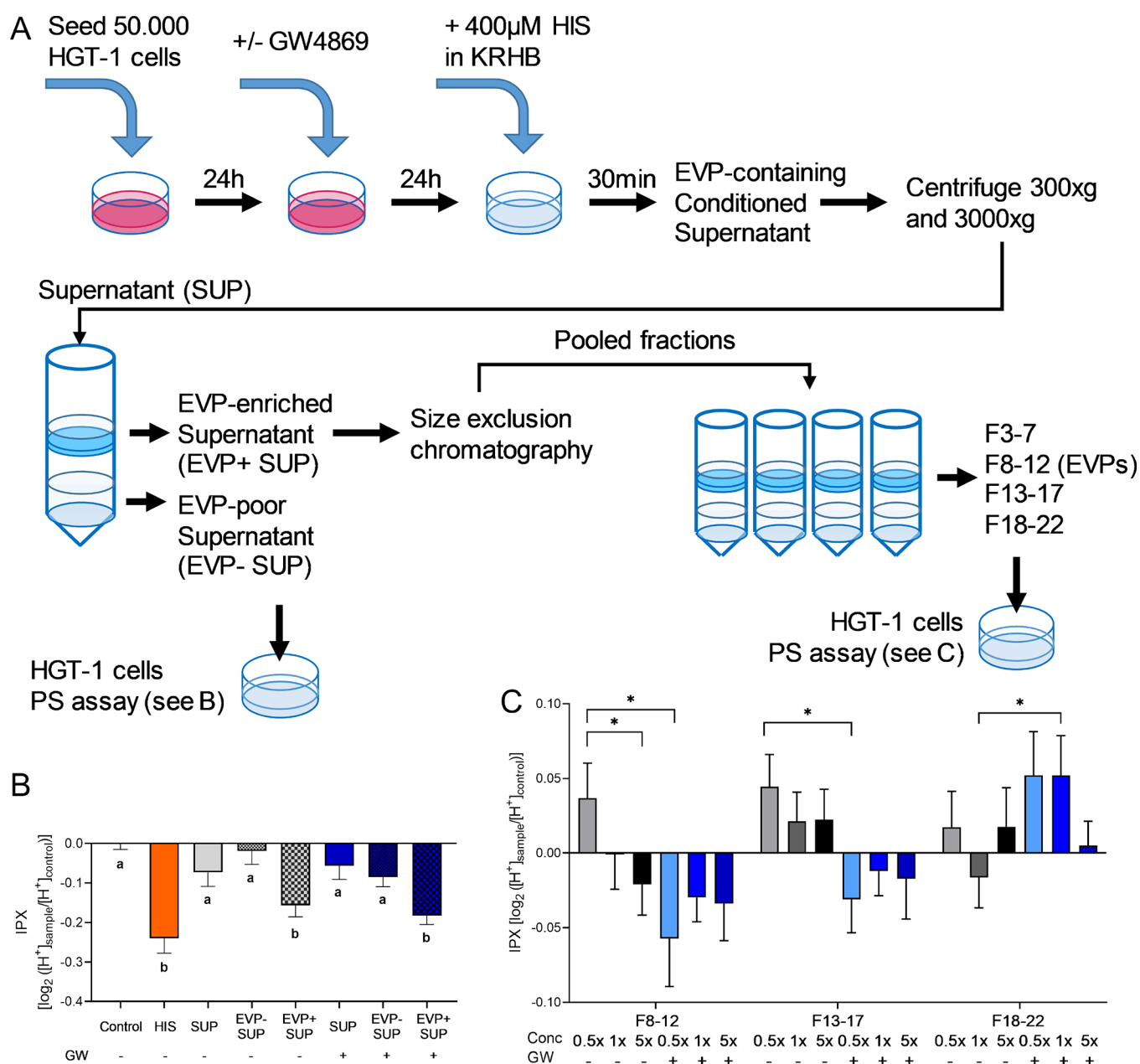
Figure 4. Effects of HGT-1 secretome and EVPs on proton secretion. (A) Schematic overview of the cell incubation and EVP isolation protocol. (B, C) Proton secretion (PS) assay, data shown as intracellular proton index (IPX) of HGT-1 cells after 10 min treated with (B) supernatant (SUP), EVP-poor supernatant (EVP− SUP), and EVP-enriched supernatant (EVP+ SUP) and (C) fractions F8−12, F13−17, F18−22 of HGT-1 cells pre-treated with or without GW4869 [10 μM] (GW) and stimulated with histamine [400 μM], compared to control cells (B) or F3−7 (C), respectively. Data are shown as mean ± SEM, $n = 4$, t.r. =3−6. Statistics: (B) one-way ANOVA on ranks versus control followed by post hoc Dunn's method, different letters indicate significant differences at a level of $p < 0.05$. (C) Student's t-test, significance indicated as * for $p < 0.05$.

techniques,[41,47−49] the inhibitory effect of GW4869 on EVP secretion has recently been verified as well by real-time, high-resolution imaging using total internal reflection fluorescence microscopy, showing that the exosome secretion activity is reduced by GW4869 treatment of HeLa cells.[30] From these results and the current literature knowledge, it can only for GW4869 be inferred that a hypothesized antagonist inhibits EVP secretion. Therefore, further experiments of the here-presented work were performed using only GW4869.

Resembling the incubation conditions tested in the proton secretion assay, HGT-1 cells were treated with GW4869 or DMSO as solvent control for 24 h and subsequently stimulated with either 400 μM histamine in KRHB or KRHB alone as

control for 10 min before cell fixation. As a result, TEM imaging of thin sections of resin-embedded HGT-1 cell layers showed no structural differences caused by the treatment with GW4869 or stimulation by histamine of cells under these conditions. HGT-1 cells mainly presented with a flat plasma membrane and microvilli were observed (see Figure 3A), but no increase in microvilli formation upon histamine stimulation became apparent. This could be due to the observation that there were no tubulovesicles present in the vicinity of plasma membranes of the HGT-1 cells, which would build the microvilli after histamine stimulation in natural parietal cells.[27] Concerning EVPs, MV secretion by membrane blebbing from lipid membrane domains (see Figure 3B) was displayed in cells

of all treatments at a similar degree. Neither a formation of exosomes within MVBs nor their fusion with the plasma membrane was observed. Consequently, no conclusions on the direct effect of GW4869 on this type of EVs and their association to proton secretion can be drawn.

Therefore, the TEM images indicate that the enhanced proton secretion after GW4869-treatment does not result from changes in the tubulovesicular structures or microvilli, supporting the hypothesis that the inhibition of EVP secretion might lead to these effects.

Additionally, interesting formations of large multivesicular structures, containing many small vesicles, at the cellular surface and in the extracellular space were discovered and should be studied for their potential functional roles in future investigations (see Figure 3C and Figure S3).

Role of HGT-1 Secretome and EVPs in Proton Secretion. Since the decrease of histamine-induced proton secretion by GW4869 could not be explained by the results obtained from TEM analysis of the cells, the direct effect of cell culture supernatants containing EVPs on proton secretion by HGT-1 cells was tested. For this purpose, HGT-1 cells were first treated with or without GW4869 for 24 h and consecutively stimulated with 400 μM histamine. After 30 min of histamine stimulation and simultaneous conditioning in KRHB, the supernatant was collected and treated according to the protocol for EVP isolation, as outlined in Figure 4A. For a first insight and to test whether the remaining histamine in the supernatant still has an effect on the cells, the EVP-conditioned supernatant, as well as the EVP-poor supernatant (filtrate, containing molecules <100 kDa) and the EVP-enriched supernatant (concentrate, containing molecules > 100 kDa), was added to untreated HGT-1 cells in order to quantitate the effects on proton secretion. The EVP-conditioned supernatant and the EVP-poor supernatant were added to the cells undiluted, while the EVP-enriched supernatant was diluted by the concentration factor for its application to HGT-1 cells. In this way, the same amount of molecules and particles secreted by HGT-1 cells from one well after histamine stimulation will act on the proton secretion of approximately the same number of untreated HGT-1 cells.

Supporting the hypothesis that EVPs could have an activating effect on proton secretion, the EVP-enriched supernatant, containing particles and molecules > 100 kDa, was demonstrated to stimulate proton secretion in HGT-1 cells (see Figure 4B). However, the EVP-enriched supernatant of the conditioned supernatant from cells treated with GW4869 showed the same effect.

Since the supernatant was conditioned during histamine stimulation of HGT-1 cells, it still contained 400 μM histamine after collection, which did not change during the concentration process by filtration, as determined by a colorimetric assay. However, this was not of concern in the EVP-enriched supernatant, since it was diluted by a factor of 20 to 52 before its addition to the cells, resulting in histamine concentrations between 8 and 20 μM, which are too low for stimulating a measurable and significant response in the proton secretion assay (see Figure 2A). However, even though the EVP-conditioned supernatant and the EVP-poor supernatant were used undiluted and therefore still contained 400 μM histamine, there was no activation of proton secretion observable from these samples. On the one hand, this might be explained by the potential presence of proton secretion-antagonists in the secretome of HGT-1 cells. On the other hand, the first

exposure of histamine to HGT-1 cells during conditioning might result in formation of histamine-protein complexes, which might not activate the histamine receptor. Since it is not clear which portion of such protein-bound histamine was detected by the used colorimetric assay, further analysis is needed to explain why histamine in the supernatant conditioned by HGT-1 cells did not stimulate proton secretion.

To further elucidate the hypothesized role of EVPs in proton secretion, EVPs were isolated from the EVP-enriched supernatant by size exclusion chromatography and the effects of the different fractions (F3−7 void volume, F8−12 EVP fraction, F13−17 intermediate size fraction, F18−22 protein fraction) were analyzed in the proton secretion assay (see Figure 4A). As performed for the EVP-enriched supernatant before, the collected fractions were also used in concentrations comparable to the concentration present per well before the isolation procedure. In detail, HGT-1 cells were treated with 0.5×, 1×, and 5× the concentration of molecules and particles that were secreted by approximately the same amount of cells during the 30 min histamine stimulation. The 1× concentration corresponded to an absolute amount of $4.54 \pm 5.42 \times 10^7$ particles per well for the EVP fraction F8−12 (mean $\pm$ SD of three biological replicates). The effects of the different fractions on proton secretion were normalized to the IPX measured when incubating HGT-1 cells with the void volume (F3−7) and shown in Figure 4C. Even though the effect size was small compared to that of 1 mM histamine, a statistically significant increase of proton secretion was measured when cells were stimulated with increasing amounts of EVPs derived from histamine-stimulated HGT-1 cells (0.5× vs 5× concentration of F8−12, one-tailed Student's t-test, $p = 0.035$). This concentration-dependent effect was not observable in cells stimulated with F13−17 or F18−22, which did not contain EVPs.

Furthermore, when comparing the proton secretion response of cells stimulated with fractions derived from untreated to GW4869-treated cells, the 0.5× concentration of the EVP fractions (F8−12) elicited a higher IPX, thereby indicating a lower proton secretion, induced by EVPs from untreated cells compared to GW-treated cells (two-tailed Student's t-test, $p = 0.022$). This difference suggests an inhibiting effect of EVPs on proton secretion, which was not observable when higher concentrations of F8−12 were analyzed. Similarly, fractions F13−17 and F18−22 also showed statistically significant differences when comparing the effects of fractions derived from untreated to GW4869-treated cells, as shown in Figure 4C.

In summary, constituents of the HGT-1-derived secretome with molecular weight > 100 kDa, including EVPs, activated proton secretion and HGT-1-derived EVPs are at least partially responsible for this effect, as discussed below.

■ DISCUSSION

Identification of HGT-1 Cell-Derived EVPs. Within this study, EVPs were isolated from HGT-1 cells, which is a cell model of gastric parietal cells. For quality assurance, the characterization of EVPs and the reporting of the used methods and results were performed according to the criteria and recommendations published by the International Society of EVs.[40] We would like to state that the methods for isolation and characterization of EVPs used in this study do not discriminate between different types of EVPs; hence, no

conclusions on the subtypes can be made. Since EVPs have been identified in EVP-conditioned culture medium of a plethora of different cell lines, including gastric cells,[50,51] the presence of EVPs in the EVP-conditioned medium of HGT-1 cells was hypothesized. As the standard cell culture medium for HGT-1 cells contains FBS, which has been demonstrated to contain EVPs,[52] the cell culture medium for EVP conditioning was ultracentrifuged before use, in order to remove or at least reduce the number of FBS-derived EVPs. The resulting unconditioned medium was subjected to the EVP isolation protocol and analyzed in parallel with the CCM, as the control experiment. Nanoparticle tracking analysis results revealed that about half of the counted particles or vesicles of the CCM were derived from the unconditioned medium, as also shown earlier.[53] This finding highlights, once again, the importance of control experiments in the field of EVP research.

Furthermore, TEM images of HGT-1 cells showed the blebbing of MVs from the cellular surface. Additionally, these images revealed multivesicular structures that show many small vesicles within one big membrane-enclosed vesicle at the surface of the cells or in the extracellular space. Since similar structures have been identified in only a few studies so far, they are described with diverse denominations as microvesicle clusters released from Nef-induced or activated T cells,[54] matrix vesicles from osteoclasts,[55] migrasomes from diverse cell types,[56] multivesicular cargo from telocytes,[57] multivesicular spheres from gastrointestinal stromal tumor cells,[58] or as small EV clusters from migrating colorectal cancer cells.[59] Based on these studies, such multivesicular structures are secreted by diverse types of cells and, therefore, might represent a new pathway of EV release or even a new class of EVs. To prove this, their characteristics, putative biosynthesis pathways and function have to be elucidated in future investigations.

Potential Role of EVPs in Gastric Function. Over the last years, many studies have revealed that EVPs play an important role in diverse cellular functions in diseased and physiological states. Also in the context of gastric cancer, EVPs have been studied extensively,[9−11] but there is still a lack of studies on their role in gastric functions. Hence, this study used a cellular model for gastric acid secretion, a central function of parietal cells,[13] and analyzed the effects of EVP inhibition on histamine-induced proton secretion. Exposure of the HGT-1 cells to the exosome inhibitor GW4869 as well as MV inhibitors imipramine hydrochloride and MβCD resulted in a decrease of the histamine-induced proton secretion, leading to the hypothesis that EVP secretion and uptake might be a novel pathway of gastric cells for self-regulation of proton secretion. This hypothesis is supported by the fact that all so far established pathways for the regulation of gastric acid secretion involve either endogenous stimuli that finally lead to the release of parietal cell-regulating signaling molecules by other cells than parietal cells or exogenous stimuli acting directly on parietal cells.[13]

Effects on Cell Membrane Structure. To analyze whether structural changes of the cells and their membranes are responsible for these effects, GW4869-treated and untreated HGT-1 cells with and without histamine stimulation were imaged by TEM. However, no such structural changes were observable after 10 min of stimulation with 400 μM histamine. The used conditions are comparable to earlier studies showing the activation of proton secretion and fusion of intracellular tubulovesicles with the plasma membrane and microvilli formation in parietal cells of piglet, rabbit, or human

gastric glands after stimulation with 1−500 μM histamine for 10−90 min.[23,26,60−62] When HGT-1 cells were first isolated from a human gastric cancer biopsy, they were reported not to have secretory vacuoles based on morphological studies using a Zeiss EM 109 electron microscope.[63] Also, the cellular distribution of H$^+$-K$^+$-ATPase, which is stored in tubulovesicles in resting parietal cells,[27] was observed within structures that were distributed throughout the cytoplasm of HGT-1 cells, but not as elaborate as in native parietal cells.[31] The transfer of H$^+$-K$^+$-ATPase to the plasma membrane in HGT-1 cells was postulated by Sandle et al.[64] who showed that omeprazole binding moieties on the cellular surface, which resembles H$^+$-K$^+$-ATPase, increased after stimulation with 1 mM histamine. Since HGT-1 cells are a gastric tumor cell line, it is possible that proton secretion upon histamine stimulation uses a different mechanism in this cell line compared to non-cancerous parietal cells. Nevertheless, HGT-1 cells are a valid model to assess the modulation of the gastric function of proton secretion,[37,38,65] while assessment of the underlying structural mechanisms in native vs tumor cells necessitates ultrastructural studies of gastric tissues.

Regarding the EVP secretion by HGT-1 cells studied here, MV blebbing from the plasma membrane was observable, although neither affected by histamine nor GW4869 treatment, as evidenced by TEM analysis. Exosomes and MVBs, on the other hand, were not observed after analysis of about 100 cells per condition (50 cells cut parallel to growth plane, 50−70 cells cut perpendicular to growth plane). Since the cell sections had a thickness of 70−90 nm and assuming a cell diameter of 10 μm and an average thickness of 3 μm, approximately 3 (parallel cut) or 1% (perpendicular cut) of each individual cell's volume was subjected to analysis in average random sectioning. Therefore, no regular imaging of exosomes and MVBs can be assumed if these structures are rarely present, similarly to the Golgi apparatus that was only rarely observed in our TEM studies, in spite of its unquestionable presence and importance as an organelle in all eukaryotic cells. Consequently, it seems that exosome formation and secretion might be a rather seldom event in HGT-1 cells in comparison to the examined MV secretion, suggesting a more important role of MVs in HGT-1 cells. In order to clarify the extent of exosome and MVB structures in HGT-1 cells, future studies involving advanced electron microscopic techniques for analyses of 3D-volumes, such as serial block face scanning electron microscopy (SEM), focused ion beam SEM, and automatic tape-collecting ultramicrotomy (ATUMtome) in combination with SEM, which are valuable tools for studying rare structural aspects, are needed.

Contrary to the findings of this work, demonstrating that EVP secretion is not affected by histamine, two previously published studies[30,66] have reported an increase in EVP secretion upon histamine stimulation in non-gastric cells. Gonzalez et al.,[66] who stimulated rat submandibular glands with 10 nM histamine for 30 min, estimated the EVP amount using their protein content and nucleotidase activity, which are bulk methods that do not quantify individual particles. Verweij et al.[30] found an increase in fusion events of MVBs with the plasma membrane, resembling the secretion of only one class of EVs, namely, exosomes, within 1−5 min after activation with 100 μM histamine in HeLa and HUVEC cells. For the HGT-1 cells studied here, neither exosomes nor their secretion could be observed in the TEM images, and with the here-used methods for EVP isolation and analysis not differentiating

between the various classes of EVs or EPs, no conclusions regarding the effect of histamine on exosome secretion by HGT-1 cells can be drawn at this point.

Functional Activity of HGT-1-Derived Secretome and EVPs in Proton Secretion. In order to further test our hypothesis that HGT-1-derived EVPs activate mechanisms regulating proton secretion of gastric cells, HGT-1 cells were stimulated with 400 μM histamine in KRHB for 30 min and the thereby conditioned KRHB supernatant was collected and concentrated by filtration to roughly separate EVPs from other components. Along the lines of the proposed theory, the EVP-enriched supernatant, which contained all particles and molecules with molecular weight > 100 kDa, including EVs and EPs, stimulated proton secretion, suggesting, for the first time, a self-regulating effect of EVPs on proton secretion in HGT-1 cells. However, the EVP-enriched supernatant of HGT-1 cells pre-incubated with GW4869 showed similar activating effects on proton secretion, indicating that EVPs other than exosomes might be the active component of the EVP-enriched supernatant, which is also supported by the TEM results, demonstrating that exosomes might be secreted in low amounts from HGT-1 cells. Nevertheless, it is also possible that the conditioning time of 30 min during histamine stimulation is simply too short to produce a difference in exosome secretion of untreated versus GW4869-treated cells that is large enough to lead to measurable differences in proton secretion because EVP-conditioning in cell culture is typically performed over a period of 24−48 h.[67] Due to the physiologically fast proton secretory response to the stimulation of the cells with histamine, such a long time of conditioning was not possible in this test setting. However, this is only a limitation of the experimental protocol and does not necessarily mean that EVP secretion under physiological conditions is too slow to affect the relatively fast reaction in a time-scale of minutes of histamine stimulation in parietal cells.[21,68] A recent study by Verweij et al.[30] showed that EVs, in particular, exosomes, are constantly released, with changes in the rate of secretion being measurable within seconds after stimulation in real-time by total internal reflection fluorescence microscopy.

To further characterize the functional activity of EVPs, as constituents of the HGT-1 secretome, the EVP-enriched supernatant was subjected to size exclusion chromatography for EVP isolation. Since filtration with a molecular weight cutoff, used for the first fractionation of the HGT-1 secretome, has a high recovery but a low specificity for EVPs,[40] the consecutive size exclusion chromatography increases EVP-specificity of the isolation procedure by further separation of EVPs from proteins and other contaminants of smaller size.[69] The functional activity of the obtained fractions was tested, and indeed, the EVP-containing fractions F8−12, derived from histamine-stimulated HGT-1 cells, elicited a concentration-dependent increase in proton secretion. This effect was not observable for fractions F13−17 or F18−22, which contained fewer EVPs and more proteins, suggesting that the activation of proton secretion is elicited by EVPs. However, F8−12 derived from GW4869-treated cells also induced an activation of proton secretion, though not concentration dependently, indicating again that exosomes might not be the chiefly responsible proton secretion-activating component of the HGT1-derived secretome. Even though the effect size of the different fractions on proton secretion in HGT-1 cells was generally small, their effects might be of biological relevance

since parietal cells continuously secrete gastric acid to restore a low pH after food ingestion to consecutively maintain this low pH in the gastric lumen.[70]

When comparing the effect on the proton secretion elicited by the EVP-enriched supernatant to that of its fractions, it is clear that part of the activity is lost during the fractionation procedure. This could be due to loss of EVPs, since the used protocol requires many steps to remove contaminants, thereby lowering the yield of EVPs. On the other hand, a multistep approach is required to increase specificity for EVPs in general, and EVs in particular, compared to other one-step approaches like ultracentrifugation or precipitation, which coisolate many more non-vesicular particles and molecules.[67] At this point, the authors want to emphasize again that the EVP fractions used for analysis of their effects on proton secretion were isolated after a conditioning time of only 30 min, which is a relatively short time period compared to that of typical EVP conditioning procedures, since proton secretion is tightly (counter-)regulated by parietal cells. With respect to EVPs, such short timespans yield a lower amount of EVPs, which adds to the problem of EVP loss during isolation procedures. In this setup, the short conditioning in KRHB with histamine stimulation yielded about 75 particles/cell, which is 13-fold less compared to the particle number isolated after 24 h from untreated HGT-1 of about 960 particles/cell after subtracting the particle number derived from the unconditioned medium. Along these lines, comparing particle concentrations with values from the literature could help to evaluate whether the isolation method yields enough vesicles for analysis. However, due to differences in EVP sources, isolation procedures, and analysis, reported values range over several orders of magnitude, as, for example, 1 μL of human blood plasma was reported to contain 200 to 10^9 EVs or EPs.[71] Thus, such comparisons are extremely difficult until a standardization of methods and detailed reporting is achieved. Furthermore, the same limitation is valid when comparing the amount of EVPs required to elicit a functional response by cells. In this case, differences in normalization approaches add another layer of variability, making conclusions on EVP functions particularly difficult.

For further elucidation of the mechanisms behind the EVP-based modulation of proton secretion in gastric cells, real-time measurements of EVP secretion, like presented by Verweij et al.,[30] are planned. Moreover, separation of different types of EVPs, e.g., by density gradient centrifugation, and functional analysis thereof will be performed in future studies.

In conclusion, we demonstrate a functional role of EVPs in the physiology of gastric parietal cells by usage of an *in vitro* cell model. Even though the exact mechanism could not be shown yet, we hypothesize that secreting cells, as parietal cells are, also use their secretome to regulate the function of their own and their adjacent parietal cells by EVPs.

■ EXPERIMENTAL PROCEDURES

Materials. DMEM Glutamax with 4 g/L glucose (Gibco) and heat inactivated fetal bovine serum (FBS, Gibco) were purchased from Thermo Fisher Scientific. Penicillin/streptomycin (10,000 units penicillin, 10 mg/mL streptomycin in 0.9% NaCl, BioReagent), trypsin/EDTA (0.5 g/mL trypsin, 0.2 g/mL EDTA in Hanks' balanced salt solution, BioReagent), Tween20, sodium azide, and sodium hydroxide from Sigma Aldrich were used, while bovine serum albumin (BSA) and dimethyl sulfoxide (DMSO, ≥99.5%, BioScience Grade)

were purchased from Carl Roth. Phosphate buffered saline (PBS, 6.7 mM PO_4, without calcium and magnesium) was acquired from Lonza. The Krebs−Ringer−HEPES buffer (KRHB) was prepared from 10 mM 4-(2-hydroxyethyl)-1-piperazineethanesulfonic acid (HEPES), 11.7 mM D-glucose, 4.7 mM KCl, 130 mM NaCl, 1.3 mM $CaCl_2$, 1.2 mM $MgSO_4$, and 1.2 mM KH_2PO_4, brought to a pH of 7.4 with 5 M KOH and filtered through 0.2 μm pore-sized filters directly before use. The cell lysis buffer consisted of RIPA-buffer with addition of SIGMAFAST protease inhibitor cocktail (tablets EDTA-free, solved in water, Sigma Aldrich) and PMSF and Na_3VO_4 at a concentration of 1 mM.

The fluorescent dye 1,5-carboxy-seminaphtorhodafluor acetoxymethyl ester (SNARF-1 AM, Thermo Fisher Scientific) was stored at −80 °C. A freshly thawed aliquot was used for each assay. Histamine (Sigma Aldrich) was dissolved in water at a concentration of 100 mM and diluted in KRHB directly before use. A turbid stock solution of 15 mM GW4869 (Sigma Aldrich) in DMSO was prepared and stored at −80 °C. For treatment of cells, the GW4869 stock was diluted and fully dissolved in medium. A 1000-fold stock solution of 25 mM of imipramine hydrochloride (Sigma Aldrich) was prepared in water and diluted in KRHB directly before use, while methyl-β-cyclodextrin (Sigma Aldrich) was solved in KRHB at a concentration of 2.5 mM and used in the assay without further dilution.

Cell Cultivation and Viability Assay. For cell culture experiments, the human gastric tumor cell line HGT-1, obtained from Dr. C. Laboisse (Laboratory of Pathological Anatomy, Nantes, Frances), was used. Cells were cultured in DMEM Glutamax, supplemented with 10% FBS and 1% penicillin/streptomycin under standard conditions at 37 °C and 5% CO_2 in a humidified incubator. For splitting and seeding, cells were detached with trypsin/EDTA.

HGT-1 cell lysates were prepared for Western blot analysis and ELISA. After detachment, 10^6 or 10^7 cells were washed twice with ice-cold PBS and lysed by addition of 300 or 500 μL lysis buffer, respectively, and homogenization by sucking through a 21 gauge needle. The lysate was then incubated at 4 °C for 30 min with agitation and then centrifuged at 14,000 × g for 15 min at 4 °C to remove cell debris. The supernatant was transferred to a new tube, and aliquots were stored at −80 °C until analysis.

For the investigation of proton secretion, the HGT-1 cells were seeded 24 h before the measurement at a density of 100,000 cells per well in black 96 well plates.[21,45] For 24 h pre-incubations with GW4869, HGT-1 cells were seeded at a density of 50,000 cells per well for a total of 48 h before the measurement to reach the same density of cells at the time point of the proton secretion assay.

The cell viability assay (MTT assay) was performed in transparent 96-well plates under the same conditions as described for the proton secretion assay. Cellular viability after the incubation with the investigated substances was tested using the 3-(4,5-dimethylthiazol-2-yl)-2,5-diphenyltetrazolium bromide (MTT) assay as described before.[72] The absorbance was measured at 570 nm and reference wavelength 650 nm using Infinite 200 Pro plate reader (Tecan, Männderdorf, Switzerland). Cell viability was calculated relative to control cells treated with medium and KRHB only.

Proton Secretion Assay. The investigation of the proton secretion in HGT 1 cells was measured by means of the intracellular pH (pH_i) using the pH-sensitive fluorescence dye SNARF 1 AM, as described before.[21,45] Briefly, HGT-1 cells were cultivated as described in the cell cultivation section. For inhibitor studies, a pre-incubation was performed with GW4869 [10 μM] or 0.07% DMSO as solvent control for 24 h (50.000 cells/ well), imipramine hydrochloride [25 μM] for 60 min, and MβCD [2.5 mM] for 15 min (100.000 cells/ well respectively) prior to washing with 100 μL KRHB and staining with 3 μM SNARF-1 AM for 35 min at standard conditions. Concentrations and incubation times of the respective inhibitors were chosen based on the literature: GW4869,[48] imipramine hydrochloride,[43] and MβCD.[44] For the investigation of the conditioned supernatant and the EVP fractions, HGT-1 cells were used directly without pre-incubation.

After washing, staining, and another washing of the cells, the subsequent stimulation was induced by histamine for the investigation with the inhibitors, or by incubation with the supernatant and EVP fractions. Fluorescence was directly measured at 580 and 640 nm emission wavelength after excitation at 488 nm using a FlexStation 3 (Molecular Devices). The intracellular pH was obtained using a pH-calibration curve, whence the intracellular H^+ concentration was calculated and a ratio between the treated and untreated cells was determined. The intracellular proton index (IPX) is calculated from the log 2 of the ratio of treated to untreated cells, whereby a low IPX-value indicates a high secretory activity.

EVP Conditioning. For EVP characterization, HGT-1 cells were cultivated in T-175 flasks (Standard TC Flask, Sarstedt) and allowed to attach for 20−24 h in standard medium before the medium was changed to the EVP-depleted cell culture medium. This EVP-depleted medium was prepared by ultracentrifugation of DMEM with 20% FBS at 100,000 × g for 18 h (Beckman Coulter Optima XPN-100 ultracentrifuge, type 45Ti rotor, 35,800 rpm). The supernatant was diluted to a final concentration of 10% FBS with serum-free DMEM and subsequently sterile filtered with vacuum sterile filtration devices (Filtropur, PES membrane with 0.2 μm pore size, Sarstedt). Cells were acclimatized in EVP-depleted medium for 24 h and after another medium change, EVP conditioning was performed for 24 h in 20 mL medium per T-175 flask. The resulting conditioned cell culture medium (CCM) from four flasks was harvested, and the EVP isolation protocol was followed. Cells were detached and stained with erythrosin B, and live and dead cells were counted with a hemocytometer.

In order to analyze the role of EVPs in the histamine-induced proton secretion, the EVP conditioning was performed in a similar procedure to the proton secretion assay protocol. HGT-1 cells (50.000 cells/ well) were seeded in a 96-well plate, allowed to attach for 24 h and then pre-incubated with GW4869 [10 μM] or 0.07% DMSO as solvent control diluted in medium for another 24 h. After washing with 100 μl KRHB, cells were stimulated with histamine and the resulting conditioned supernatant was collected after 30 min. The supernatant of 600 wells was pooled to reach a final volume of 30 mL of conditioned KRHB supernatant from approximately 10^7 cells, and the EVP isolation protocol was followed.

EVP Isolation. A total volume of 80 mL of CCM, as well as unconditioned EVP-depleted medium as control, or 30 mL of conditioned KRHB supernatant from the different incubations, was centrifuged at 300 × g and 3000 × g for 10 min each to remove cells and cell debris. The resulting supernatant was

concentrated with Amicon Ultra-15 centrifugal filter devices (MW-cutoff 100 kDa, Merck Millipore), and the concentrate was subsequently used for EVP purification by size exclusion chromatography with qEV2/70 nm columns (IZON Science). The CCM was concentrated to a volume below 4 mL (27−60× concentration) and loaded onto two columns to avoid overloading due to high protein concentration, while the conditioned KRHB supernatant was concentrated to a volume below 2 mL (20−52× concentration) and loaded onto one column. Aliquots of the conditioned KRHB solution before concentration (supernatant), the concentrate (EVP-enriched supernatant), and the filtrate (EVP-poor supernatant) were directly analyzed in the proton secretion assay. The size exclusion chromatography was performed according to the manufacturer's instructions. PBS was degassed by sonication for 15 min and used as running buffer, qEV columns were reused up to five times, cleaned with 0.5 M NaOH in between and stored in PBS with 0.05% w/v sodium azide at 4 °C. After initial testing of the size exclusion chromatography and collection of all fractions individually, fractions of interest were collected together and again concentrated with Amicon Ultra-4 centrifugal filter devices (MW-cutoff 4 kDa, Millipore) to a volume of 150−300 μL. The Amicon Ultra filters were blocked with PBS supplemented with 0.1% BSA and 0.05% Tween20 directly before usage. The resulting concentrates of EVPs and other fractions were analyzed directly by nanoparticle tracking analysis and subsequently stored at −80 °C until further use.

Nanoparticle Tracking Analysis. The ZetaView PMX 120-Z equipped with a 520 nm laser (Particle Metrix) was used for the determination of particle concentration, size distribution, and zeta potential. Before starting measurements, the instrument was calibrated with polystyrene standard beads according to the manufacturer's instructions. The instrument settings (pre- and post-acquisition parameters) were optimized for the measurement of small particles, like EVPs, and kept constant over all measurements: shutter 70, sensitivity 84, frame rate 30, min. brightness 20, and trace length 15. All measurements were performed in dilutions with PBS, reaching a particle number of about 100−200 particles per frame with the optimized settings. Three measurements over all 11 positions of the flow cell were performed for concentration determination. A minimum of 1000 particles were analyzed for size and zeta potential analysis. The software ZetaView was used for analysis.

Western Blot and ELISA. The protein concentration in cell lysates and the concentrated fractions was determined by the Bradford assay. SDS-PAGE and Western blotting was performed as previously described.[73,74] After boiling in 6× Laemmli buffer at 95 °C for 5 min, either 10 μg of total protein or the maximal volume of 18 μL of those samples with lower protein amounts was loaded on a 12% polyacrylamide SDS-gel and 3 μL of color prestained protein standard, broad range 11−245 or 10−250 kDa (New England Biolabs), was used. After protein separation, proteins were transferred by semi-dry blotting to PVDF membranes, which were then blocked for 1 h in 5% skim milk in Tris buffered saline with 0.1% Tween20 (TBS-T). All antibody dilutions were prepared in the same blocking buffer, and details on the antibodies used are given in Table S1. The blocked membranes were incubated with primary antibodies overnight at 4 °C. After washing with TBS-T, secondary antibody dilutions were added and incubated for 1 h at room temperature. After washing with TBS-T again,

membranes were incubated with SignalFire chemiluminescence reagent (CST Cell Signaling) and chemiluminescence was detected with the Fusion FX7 device (Vilber Lourmat). Image analysis was performed with the software ImageJ.

For the analysis of the H^+-K^+-ATPase α-subunit, an ELISA kit (DL-ATP4a-Hu by DL Develop) was used according to the manufacturer's instructions. Cell lysates and the concentrated fractions were diluted 10-fold for analysis.

Transmission Electron Microscopy (TEM). Cryo TEM was used to examine the vesicular structure and prove the presence of a lipid bilayer of the purified particles. For this purpose, EVP samples were analyzed by the Electron Microscopy Facility of the Vienna BioCenter Core Facilities GmbH according to the following procedure. Quantifoil Cu 400 mesh R1.2/1.3 holey carbon grids (Großlöbichau, Germany) and 400 mesh copper-palladium grids with a self-made 4 nm-thick continuous carbon film were glow discharged for 1 min at −25 mA with a Bal-Tec (Balzers, Liechtenstein) SCD005 glow discharger and loaded into a grid plunger Leica GP (Leica Microsystems, Vienna, Austria) with the climate chamber set at 70% relative humidity and 4 °C. Sample aliquots of 4 μL were pipetted onto the carbon side of the grid and front-side blotted with Whatman filter paper #1 (Little Chalfont, Great Britain) for 1−4 s using the instrument's sensor function and vitrified by plunge freezing into liquid ethane at approximately −180 °C. Grids were visualized at a Glacios cryo-transmission electron microscope (Thermo Scientific, USA) equipped with an X-FEG and a Falcon3 direct electron detector (4096 x 4096 pixels). Using the SerialEM data acquisition software[75] and operating in low-dose mode, digital images were recorded in linear mode of the Falcon3 camera at magnifications of 5300 (pixel size: 27.5 Å, defocus: −50 μm, dose: 0.2 e/Å2), 28,000 (pixel size: 5.2 Å, defocus: −8 μm, dose: 10 e/Å2), and 150,000 (pixel size: 0.98 Å, defocus: −3 μm, dose: 60 e/Å2).

TEM with chemical fixation was used for examination of membrane structures in whole HGT-1 cell layers. For this purpose, cells were cultivated on Aclar discs, 119 μm in thickness and 13 mm in diameter, which were punched out from Aclar 33C foil (Science Services GmbH, Munich, Germany) using an appropriate punch tool (no. 77850-12; EMS, Hatfield, PA). Before usage, the discs were sterilized with 70% ethanol and incubated in serum-free medium at 37 °C for several hours. HGT-1 cells (100.000 cells/well) were seeded on Aclar discs in 24-well plates, and after attachment of the cells for 20−24 h in 600 μL medium per well at 37 °C, cells were incubated with 10 μM GW4869 or 0.07% DMSO (solvent control) diluted in 600 μL of medium for 24 h. Cells were then washed with 600 μL of freshly filtered KRHB and treated with 600 μL of 400 μM histamine diluted in KRHB or KRHB alone for 10 min. The solution was removed, and the cells were chemically fixed with 2.5% glutaraldehyde in 0.1 M sodium cacodylate buffer, pH 7.3, for 45 min.

For resin embedding, the cells remained attached to the Aclar discs throughout the procedure. After 3 times washing in buffer, cells were osmicated with 1% osmium tetroxide in 0.1 M sodium cacodylate buffer, pH 7.3, for 1 h 30 min. Subsequently, the Aclar discs with the cells attached were washed with buffer and transferred in 6-well plates with solvent-resistant polypropylene inserts. The cells were dehydrated in a series of ethanol (30, 50, 70, and 95% for 10 min each; 2 times 100% for 5 min each). Subsequently, ethanol was replaced by 100% acetone, followed by an

infiltration schedule with the following mixtures of epoxy resin Agar 100 (Agar Scientific Ltd., Stansted, UK) and acetone: one part resin/two parts acetone for 15 min, one part resin/one part acetone for 15 min, and two parts resin/one part acetone for 45 min. Prior to infiltration with drops of pure resin, the Aclar discs were transferred to glass slides with cells facing up. After 3 h infiltration with pure resin, Eppendorf tubes with their bottoms and lids cut off were placed inversely onto each Aclar disc. After polymerization in an oven at 65 °C for about 3 h, the Eppendorf tubes stuck to the Aclar discs. Consequently, the tubes were filled up with resin without risking leakage. After final polymerization in the oven, the resin blocks confined by the Eppendorf tubes were detached from the glass slide with the help of liquid nitrogen. Once the plastics of the Eppendorf tubes was cut away with a razor blade, the Aclar discs could be peeled off easily from the resin block.

Prior to sectioning, the resin blocks were cut with a hand saw longitudinally, resulting in four samples, each containing a quarter segment of the circular cell layer. If sectioning of the cells perpendicularly to the growth plane was intended, the samples were glued on resin blocks, accordingly. Ultrathin sections of the embedded cell layers (70−90 nm in thickness) were cut with an ultramicrotome Ultracut S (LEICA Microsystems, Austria) by using a diamond knife (Diatome, Nidau, Switzerland), placed on 200-mesh copper grids, and contrasted with 4% neodymium(III)-acetate[76] for 50 min followed by lead citrate for 8 min, prior to analyses in a TEM ZEISS Libra 120 (ZEISS, Germany) at 120 kV. Images were acquired by using a bottom stage digital camera, TRS (4 megapixel), and ImageSp-professional software (Tröndle, Moorenweis, Germany).

Histamine Assay. To determine the concentration of histamine in the conditioned KRHB supernatant, the filtrate, and the concentrate, an enzymatic histamine assay with colorimetric detection was used and performed according to the manufacturer's instructions (ab235630, Abcam).

Quantification and Statistical Analysis. Statistical analysis was performed with Excel, SigmaPlot (Software Version 13.0), and GraphPad Prism (Software Version 8). Data are shown as mean ± SEM or mean ± SD. Using the Nalimov test, non-confident values were identified and excluded. The numbers of biological and technical replicates for each experiment are specified in the result section. For all data, tests for normality (Shapiro−Wilk) and equal variances (Brown−Forsythe) were performed and the appropriate statistical tests were conducted. Comparisons between two different treatments with normally distributed data were performed using one- and two-tailed Student's t-test for equal variances, and significant differences are indicated with *. For multiple comparisons, a one-way ANOVA was performed with a Holm−Sidak post hoc test for normally distributed data and a one-way ANOVA on Ranks with post hoc Dunn's method for not normally distributed data. Different letters indicate significant differences evaluated by one-way ANOVA.

ASSOCIATED CONTENT

Data Availability Statement
The data presented in this study are available in this article and the Supporting Information. Further information and requests for resources may be directed to and will be fulfilled by the corresponding author Agnes Mistlberger-Reiner, PhD (agnes. mistlberger-reiner@univie.ac.at).

Supporting Information
The Supporting Information is available free of charge at https://pubs.acs.org/doi/10.1021/acsomega.2c06442.

> (Table S1) Primary and secondary antibodies used in Western blot analysis; (Figure S1) particle concentration and protein concentration of pooled and concentrated fractions; (Figure S2) intracellular proton index (IPX) of HGT-1 cells treated with 1 mM histamine; (Figure S3) additional TEM images of multivesicular structures from HGT-1 cells; and (Figure S4) images of total Western blot membranes depicted in Figure 1 (PDF)

AUTHOR INFORMATION

Corresponding Author
Agnes Mistlberger-Reiner − *Department of Physiological Chemistry, Faculty of Chemistry, University of Vienna, Vienna 1090, Austria;* orcid.org/0000-0002-7077-1199; Email: agnes.mistlberger-reiner@univie.ac.at

Authors
Sonja Sterneder − *Department of Physiological Chemistry, Faculty of Chemistry, University of Vienna, Vienna 1090, Austria*

Siegfried Reipert − *Core Facility Cell Imaging and Ultrastructure Research, University of Vienna, Vienna 1030, Austria*

Sara Wolske − *Department of Physiological Chemistry, Faculty of Chemistry, University of Vienna, Vienna 1090, Austria*

Veronika Somoza − *Department of Physiological Chemistry, Faculty of Chemistry, University of Vienna, Vienna 1090, Austria; Leibniz-Institute for Food Systems Biology at the Technical University of Munich, Freising 85354, Germany; Nutritional Systems Biology, Technical University of Munich, Freising 85354, Germany*

Complete contact information is available at:
https://pubs.acs.org/10.1021/acsomega.2c06442

Author Contributions
Conceptualization was done by A.M.-R. and V.S.; formal analysis was done by A.M.-R., S.S., and S.R.; funding acquisition was done by V.S.; investigation was done by A.M.-R., S.S., S.W., and S.R.; methodology was done by A.M.-R.; project administration was done by A.M.-R.; supervision was done by V.S.; validation was done by A.M.-R.; visualization was done by A.M.-R. and S.S.; writing of the original draft was done by A.M.-R., S.S., S.R.; reviewing & editing were done by A.M.-R. and V.S.

Notes
The authors declare no competing financial interest.

ABBREVIATIONS

CCM EVP-conditioned cell culture medium
Ctrl DMEM EVP-unconditioned medium
EP extracellular particle
EV extracellular vesicle
EVP extracellular vesicles and particles
IPX intracellular proton index
MβCD methyl-β-cyclodextrin
MV microvesicle
MVB multivesicular body
TEM transmission electron microscopy

REFERENCES

(1) Harding, C.; Heuser, J.; Stahl, P. Receptor-mediated endocytosis of transferrin and recycling of the transferrin receptor in rat reticulocytes. *J. Cell Biol.* **1983**, *97*, 329−339.

(2) Pan, B. T.; Johnstone, R. M. Fate of the transferrin receptor during maturation of sheep reticulocytes in vitro: selective externalization of the receptor. *Cell* **1983**, *33*, 967−978.

(3) van Niel, G.; D'Angelo, G.; Raposo, G. Shedding light on the cell biology of extracellular vesicles. *Nat. Rev. Mol. Cell Biol.* **2018**, *19*, 213−228.

(4) Zhang, Q.; Higginbotham, J. N.; Jeppesen, D. K.; Yang, Y. P.; Li, W.; McKinley, E. T.; Graves-Deal, R.; Ping, J.; Britain, C. M.; Dorsett, K. A.; Hartman, C. L.; Ford, D. A.; Allen, R. M.; Vickers, K. C.; Liu, Q.; Franklin, J. L.; Bellis, S. L.; Coffey, R. J. Transfer of Functional Cargo in Exomeres. *Cell Rep.* **2019**, *27*, 940−954.e6 e6.

(5) Zhang, Q.; Jeppesen, D. K.; Higginbotham, J. N.; Graves-Deal, R.; Trinh, V. Q.; Ramirez, M. A.; Sohn, Y.; Neininger, A. C.; Taneja, N.; McKinley, E. T.; Niitsu, H.; Cao, Z.; Evans, R.; Glass, S. E.; Ray, K. C.; Fissell, W. H.; Hill, S.; Rose, K. L.; Huh, W. J.; Washington, M. K.; Ayers, G. D.; Burnette, D. T.; Sharma, S.; Rome, L. H.; Franklin, J. L.; Lee, Y. A.; Liu, Q.; Coffey, R. J. Supermeres are functional extracellular nanoparticles replete with disease biomarkers and therapeutic targets. *Nat. Cell Biol.* **2021**, *23*, 1240−1254.

(6) Tabet, F.; Vickers, K. C.; Cuesta Torres, L. F.; Wiese, C. B.; Shoucri, B. M.; Lambert, G.; Catherinet, C.; Prado-Lourenco, L.; Levin, M. G.; Thacker, S.; Sethupathy, P.; Barter, P. J.; Remaley, A. T.; Rye, K. A. HDL-transferred microRNA-223 regulates ICAM-1 expression in endothelial cells. *Nat. Commun.* **2014**, *5*, 3292.

(7) Yáñez-Mó, M.; Siljander, P. R.-M.; Andreu, Z.; Zavec, A. B.; Borràs, F. E.; Buzas, E. I.; Buzas, K.; Casal, E.; Cappello, F.; Carvalho, J.; Colás, E.; Cordeiro-da Silva, A.; Fais, S.; Falcon-Perez, J. M.; Ghobrial, I. M.; Giebel, B.; Gimona, M.; Graner, M.; Gursel, I.; Gursel, M.; Heegaard, N. H.; Hendrix, A.; Kierulf, P.; Kokubun, K.; Kosanovic, M.; Kralj-Iglic, V.; Krämer-Albers, E. M.; Laitinen, S.; Lässer, C.; Lener, T.; Ligeti, E.; Linē, A.; Lipps, G.; Llorente, A.; Lötvall, J.; Manček-Keber, M.; Marcilla, A.; Mittelbrunn, M.; Nazarenko, I.; Nolte-'t Hoen, E. N.; Nyman, T. A.; O'Driscoll, L.; Olivan, M.; Oliveira, C.; Pállinger, É.; Del Portillo, H. A.; Reventós, J.; Rigau, M.; Rohde, E.; Sammar, M.; Sánchez-Madrid, F.; Santarém, N.; Schallmoser, K.; Ostenfeld, M. S.; Stoorvogel, W.; Stukelj, R.; Van der Grein, S. G.; Vasconcelos, M. H.; Wauben, M. H. M.; De Wever, O. Biological properties of extracellular vesicles and their physiological functions. *J. Extracell. Vesicles* **2015**, *4*, 27066.

(8) Kalluri, R.; LeBleu, V. S. The biology, function, and biomedical applications of exosomes. *Science* **2020**, *367*, No. eaau6977.

(9) Fu, M.; Gu, J.; Jiang, P.; Qian, H.; Xu, W.; Zhang, X. Exosomes in gastric cancer: roles, mechanisms, and applications. *Mol. Cancer* **2019**, *18*, 41.

(10) Huang, T.; Song, C.; Zheng, L.; Xia, L.; Li, Y.; Zhou, Y. The roles of extracellular vesicles in gastric cancer development, microenvironment, anti-cancer drug resistance, and therapy. *Mol. Cancer* **2019**, *18*, 62.

(11) Kahroba, H.; Hejazi, M. S.; Samadi, N. Exosomes: from carcinogenesis and metastasis to diagnosis and treatment of gastric cancer. *Cell. Mol. Life Sci.* **2019**, *76*, 1747−1758.

(12) Kagota, S.; Taniguchi, K.; Lee, S. W.; Ito, Y.; Kuranaga, Y.; Hashiguchi, Y.; Inomata, Y.; Imai, Y.; Tanaka, R.; Tashiro, K.; Kawai, M.; Akao, Y.; Uchiyama, K. Analysis of Extracellular Vesicles in Gastric Juice from Gastric Cancer Patients. *Int. J. Mol. Sci.* **2019**, *20*, 953.

(13) Engevik, A. C.; Kaji, I.; Goldenring, J. R. The Physiology of the Gastric Parietal Cell. *Physiol. Rev.* **2020**, *100*, 573−602.

(14) Black, J. W.; Duncan, W. A. M.; Durant, C. J.; Ganellin, C. R.; Parsons, E. M. Definition and antagonism of histamine H2-receptors. *Nature* **1972**, *236*, 385−390.

(15) Cabero, J. L.; Li, Z. Q.; Mårdh, S. Gastrin potentiates histamine-stimulated aminopyrine accumulation in isolated rat parietal cells. *Am. J. Physiol.* **1991**, *261*, G621−G627.

(16) Soll, A. H. Secretagogue stimulation of [14C]aminopyrine accumulation by isolated canine parietal cells. *Am. J. Physiol.* **1980**, *238*, G366−G375.

(17) Lindstrom, E.; Bjorkqvist, M.; Boketoft, A.; Chen, D.; Zhao, C. M.; Kimura, K.; Hakanson, R. Neurohormonal regulation of histamine and pancreastatin secretion from isolated rat stomach ECL cells. *Regul. Pept.* **1997**, *71*, 73−86.

(18) Pfeiffer, A.; Rochlitz, H.; Noelke, B.; Tacke, R.; Moser, U.; Mutschler, E.; Lambrecht, G. Muscarinic receptors mediating acid secretion in isolated rat gastric parietal cells are of M3 type. *Gastroenterology* **1990**, *98*, 218−222.

(19) Park, J.; Chiba, T.; Yamada, T. Mechanisms for direct inhibition of canine gastric parietal cells by somatostatin. *J. Biol. Chem.* **1987**, *262*, 14190−14196.

(20) Wyatt, M. A.; Jarvie, E.; Feniuk, W.; Humphrey, P. P. A. Somatostatin sst2 receptor-mediated inhibition of parietal cell function in rat isolated gastric mucosa. *Br. J. Pharmacol.* **1996**, *119*, 905−910.

(21) Liszt, K. I.; Ley, J. P.; Lieder, B.; Behrens, M.; Stöger, V.; Reiner, A.; Hochkogler, C. M.; Köck, E.; Marchiori, A.; Hans, J.; Widder, S.; Krammer, G.; Sanger, G. J.; Somoza, M. M.; Meyerhof, W.; Somoza, V. Caffeine induces gastric acid secretion via bitter taste signaling in gastric parietal cells. *Proc. Natl. Acad. Sci. U. S. A.* **2017**, *114*, E6260−E6269.

(22) Chew, C. S. Parietal cell protein kinases. Selective activation of type I cAMP-dependent protein kinase by histamine. *J. Biol. Chem.* **1985**, *260*, 7540−7550.

(23) Chew, C. S.; Hersey, S. J.; Sachs, G.; Berglindh, T. Histamine responsiveness of isolated gastric glands. *Am. J. Physiol.* **1980**, *238*, G312−G320.

(24) Negulescu, P. A.; Reenstra, W. W.; Machen, T. E. Intracellular Ca requirements for stimulus-secretion coupling in parietal cell. *Am. J. Physiol.* **1989**, *256*, C241−C251.

(25) Chew, C. S.; Brown, M. R. Release of intracellular Ca2+ and elevation of inositol trisphosphate by secretagogues in parietal and chief cells isolated from rabbit gastric mucosa. *Biochim. Biophys. Acta* **1986**, *888*, 116−125.

(26) Forte, T. M.; Machen, T. E.; Forte, J. G. Ultrastructural Changes in Oxyntic Cells Associated with Secretory Function: A Membrane-Recycling Hypothesis. *Gastroenterology* **1977**, *73*, 941−955.

(27) Forte, J. G.; Zhu, L. Apical recycling of the gastric parietal cell H, K-ATPase. *Annu. Rev. Physiol.* **2010**, *72*, 273−296.

(28) Alonso, R.; Rodriguez, M. C.; Pindado, J.; Merino, E.; Mérida, I.; Izquierdo, M. Diacylglycerol kinase alpha regulates the secretion of lethal exosomes bearing Fas ligand during activation-induced cell death of T lymphocytes. *J. Biol. Chem.* **2005**, *280*, 28439−28450.

(29) Conrad, K. P.; Tuna, K. M.; Mestre, C. T.; Banwatt, E. S.; Alli, A. A. Activation of multiple receptors stimulates extracellular vesicle release from trophoblast cells. *Physiol. Rep.* **2020**, *8*, No. e14592.

(30) Verweij, F. J.; Bebelman, M. P.; Jimenez, C. R.; Garcia-Vallejo, J. J.; Janssen, H.; Neefjes, J.; Knol, J. C.; de Goeij-de Haas, R.; Piersma, S. R.; Baglio, S. R.; Verhage, M.; Middeldorp, J. M.; Zomer,

A.; van Rheenen, J.; Coppolino, M. G.; Hurbain, I.; Raposo, G.; Smit, M. J.; Toonen, R. F. G.; van Niel, G.; Pegtel, D. M. Quantifying exosome secretion from single cells reveals a modulatory role for GPCR signaling. *J. Cell Biol.* **2018**, *217*, 1129−1142.

(31) Carmosino, M.; Procino, G.; Casavola, V.; Svelto, M.; Valenti, G. The cultured human gastric cells HGT-1 express the principal transporters involved in acid secretion. *Pflug. Arch.* **2000**, *440*, 871−880.

(32) Weiss, C.; Rubach, M.; Lang, R.; Seebach, E.; Blumberg, S.; Frank, O.; Hofmann, T.; Somoza, V. Measurement of the intracellular ph in human stomach cells: a novel approach to evaluate the gastric acid secretory potential of coffee beverages. *J. Agric. Food Chem.* **2010**, *58*, 1976−1985.

(33) Rubach, M.; Lang, R.; Skupin, C.; Hofmann, T.; Somoza, V. Activity-guided fractionation to characterize a coffee beverage that effectively down-regulates mechanisms of gastric acid secretion as compared to regular coffee. *J. Agric. Food Chem.* **2010**, *58*, 4153−4161.

(34) Rubach, M.; Lang, R.; Seebach, E.; Somoza, M. M.; Hofmann, T.; Somoza, V. Multi-parametric approach to identify coffee components that regulate mechanisms of gastric acid secretion. *Mol. Nutr. Food Res.* **2012**, *56*, 325−335.

(35) Sterneder, S.; Stoeger, V.; Dugulin, C. A.; Liszt, K. I.; Di Pizio, A.; Korntheuer, K.; Dunkel, A.; Eder, R.; Ley, J. P.; Somoza, V. Astringent Gallic Acid in Red Wine Regulates Mechanisms of Gastric Acid Secretion via Activation of Bitter Taste Sensing Receptor TAS2R4. *J. Agric. Food Chem.* **2021**, *69*, 10550−10561.

(36) Zopun, M.; Liszt, K. I.; Stoeger, V.; Behrens, M.; Redel, U.; Ley, J. P.; Hans, J.; Somoza, V. Human Sweet Receptor T1R3 is Functional in Human Gastric Parietal Tumor Cells (HGT-1) and Modulates Cyclamate and Acesulfame K-Induced Mechanisms of Gastric Acid Secretion. *J. Agric. Food Chem.* **2018**, *66*, 4842−4852.

(37) Liszt, K. I.; Walker, J.; Somoza, V. Identification of organic acids in wine that stimulate mechanisms of gastric acid secretion. *J. Agric. Food Chem.* **2012**, *60*, 7022−7030.

(38) Rubach, M.; Lang, R.; Bytof, G.; Stiebitz, H.; Lantz, I.; Hofmann, T.; Somoza, V. A dark brown roast coffee blend is less effective at stimulating gastric acid secretion in healthy volunteers compared to a medium roast market blend. *Mol. Nutr. Food Res.* **2014**, *58*, 1370−1373.

(39) Beltran, L. R.; Sterneder, S.; Hasural, A.; Paetz, S.; Hans, J.; Ley, J. P.; Somoza, V. Reducing the Bitter Taste of Pharmaceuticals Using Cell-Based Identification of Bitter-Masking Compounds. *Pharmaceuticals (Basel)* **2022**, *15*, 317.

(40) Thery, C.; Witwer, K. W.; Aikawa, E.; Alcaraz, M. J.; Anderson, J. D.; Andriantsitohaina, R.; Antoniou, A.; Arab, T.; Archer, F.; Atkin-Smith, G. K.; Ayre, D. C.; Bach, J. M.; Bachurski, D.; Baharvand, H.; Balaj, L.; Baldacchino, S.; Bauer, N. N.; Baxter, A. A.; Bebawy, M.; Beckham, C.; Bedina Zavec, A.; Benmoussa, A.; Berardi, A. C.; Bergese, P.; Bielska, E.; Blenkiron, C.; Bobis-Wozowicz, S.; Boilard, E.; Boireau, W.; Bongiovanni, A.; Borras, F. E.; Bosch, S.; Boulanger, C. M.; Breakefield, X.; Breglio, A. M.; Brennan, M. A.; Brigstock, D. R.; Brisson, A.; Broekman, M. L.; Bromberg, J. F.; Bryl-Gorecka, P.; Buch, S.; Buck, A. H.; Burger, D.; Busatto, S.; Buschmann, D.; Bussolati, B.; Buzas, E. I.; Byrd, J. B.; Camussi, G.; Carter, D. R.; Caruso, S.; Chamley, L. W.; Chang, Y. T.; Chen, C.; Chen, S.; Cheng, L.; Chin, A. R.; Clayton, A.; Clerici, S. P.; Cocks, A.; Cocucci, E.; Coffey, R. J.; Cordeiro-da-Silva, A.; Couch, Y.; Coumans, F. A.; Coyle, B.; Crescitelli, R.; Criado, M. F.; D'Souza-Schorey, C.; Das, S.; Datta Chaudhuri, A.; de Candia, P.; De Santana, E. F.; De Wever, O.; Del Portillo, H. A.; Demaret, T.; Deville, S.; Devitt, A.; Dhondt, B.; Di Vizio, D.; Dieterich, L. C.; Dolo, V.; Dominguez Rubio, A. P.; Dominici, M.; Dourado, M. R.; Driedonks, T. A.; Duarte, F. V.; Duncan, H. M.; Eichenberger, R. M.; Ekstrom, K.; El Andaloussi, S.; Elie-Caille, C.; Erdbrugger, U.; Falcon-Perez, J. M.; Fatima, F.; Fish, J. E.; Flores-Bellver, M.; Forsonits, A.; Frelet-Barrand, A.; Fricke, F.; Fuhrmann, G.; Gabrielsson, S.; Gamez-Valero, A.; Gardiner, C.; Gartner, K.; Gaudin, R.; Gho, Y. S.; Giebel, B.; Gilbert, C.; Gimona, M.; Giusti, I.; Goberdhan, D. C.; Gorgens, A.; Gorski, S. M.; Greening, D. W.; Gross, J. C.; Gualerzi, A.; Gupta, G. N.; Gustafson, D.; Handberg, A.; Haraszti, R. A.; Harrison, P.; Hegyesi, H.; Hendrix, A.; Hill, A. F.; Hochberg, F. H.; Hoffmann, K. F.; Holder, B.; Holthofer, H.; Hosseinkhani, B.; Hu, G.; Huang, Y.; Huber, V.; Hunt, S.; Ibrahim, A. G.; Ikezu, T.; Inal, J. M.; Isin, M.; Ivanova, A.; Jackson, H. K.; Jacobsen, S.; Jay, S. M.; Jayachandran, M.; Jenster, G.; Jiang, L.; Johnson, S. M.; Jones, J. C.; Jong, A.; Jovanovic-Talisman, T.; Jung, S.; Kalluri, R.; Kano, S. I.; Kaur, S.; Kawamura, Y.; Keller, E. T.; Khamari, D.; Khomyakova, E.; Khvorova, A.; Kierulf, P.; Kim, K. P.; Kislinger, T.; Klingeborn, M.; Klinke, D. J., II; Kornek, M.; Kosanovic, M. M.; Kovacs, A. F.; Kramer-Albers, E. M.; Krasemann, S.; Krause, M.; Kurochkin, I. V.; Kusuma, G. D.; Kuypers, S.; Laitinen, S.; Langevin, S. M.; Languino, L. R.; Lannigan, J.; Lasser, C.; Laurent, L. C.; Lavieu, G.; Lazaro-Ibanez, E.; Le Lay, S.; Lee, M. S.; Lee, Y. X. F.; Lemos, D. S.; Lenassi, M.; Leszczynska, A.; Li, I. T.; Liao, K.; Libregts, S. F.; Ligeti, E.; Lim, R.; Lim, S. K.; Line, A.; Linnemannstons, K.; Llorente, A.; Lombard, C. A.; Lorenowicz, M. J.; Lorincz, A. M.; Lotvall, J.; Lovett, J.; Lowry, M. C.; Loyer, X.; Lu, Q.; Lukomska, B.; Lunavat, T. R.; Maas, S. L.; Malhi, H.; Marcilla, A.; Mariani, J.; Mariscal, J.; Martens-Uzunova, E. S.; Martin-Jaular, L.; Martinez, M. C.; Martins, V. R.; Mathieu, M.; Mathivanan, S.; Maugeri, M.; McGinnis, L. K.; McVey, M.; Meckes, D. G., Jr.; Meehan, K. L.; Mertens, I.; Minciacchi, V. R.; Moller, M.; Moller Jorgensen, M.; Morales-Kastresana, A.; Morhayim, J.; Mullier, F.; Muraca, M.; Musante, L.; Mussack, V.; Muth, D. C.; Myburgh, K. H.; Najrana, T.; Nawaz, M.; Nazarenko, I.; Nejsum, P.; Neri, C.; Neri, T.; Nieuwland, R.; Nimrichter, L.; Nolan, J. P.; Nolte'T Hoen, E. N.; Noren Hooten, N.; O'Driscoll, L.; O'Grady, T.; O'Loghlen, A.; Ochiya, T.; Olivier, M.; Ortiz, A.; Ortiz, L. A.; Osteikoetxea, X.; Ostergaard, O.; Ostrowski, M.; Park, J.; Pegtel, D. M.; Peinado, H.; Perut, F.; Pfaffl, M. W.; Phinney, D. G.; Pieters, B. C.; Pink, R. C.; Pisetsky, D. S.; Pogge von Strandmann, E.; Polakovicova, I.; Poon, I. K.; Powell, B. H.; Prada, I.; Pulliam, L.; Quesenberry, P.; Radeghieri, A.; Raffai, R. L.; Raimondo, S.; Rak, J.; Ramirez, M. I.; Raposo, G.; Rayyan, M. S.; Regev-Rudzki, N.; Ricklefs, F. L.; Robbins, P. D.; Roberts, D. D.; Rodrigues, S. C.; Rohde, E.; Rome, S.; Rouschop, K. M.; Rughetti, A.; Russell, A. E.; Saa, P.; Sahoo, S.; Salas-Huenuleo, E.; Sanchez, C.; Saugstad, J. A.; Saul, M. J.; Schiffelers, R. M.; Schneider, R.; Schoyen, T. H.; Scott, A.; Shahaj, E.; Sharma, S.; Shatnyeva, O.; Shekari, F.; Shelke, G. V.; Shetty, A. K.; Shiba, K.; Siljander, P. R.; Silva, A. M.; Skowronek, A.; Snyder, O. L., 2nd; Soares, R. P.; Sodar, B. W.; Soekmadji, C.; Sotillo, J.; Stahl, P. D.; Stoorvogel, W.; Stott, S. L.; Strasser, E. F.; Swift, S.; Tahara, H.; Tewari, M.; Timms, K.; Tiwari, S.; Tixeira, R.; Tkach, M.; Toh, W. S.; Tomasini, R.; Torrecilhas, A. C.; Tosar, J. P.; Toxavidis, V.; Urbanelli, L.; Vader, P.; van Balkom, B. W.; van der Grein, S. G.; Van Deun, J.; van Herwijnen, M. J.; Van Keuren-Jensen, K.; van Niel, G.; van Royen, M. E.; van Wijnen, A. J.; Vasconcelos, M. H.; Vechetti, I. J., Jr.; Veit, T. D.; Vella, L. J.; Velot, E.; Verweij, F. J.; Vestad, B.; Vinas, J. L.; Visnovitz, T.; Vukman, K. V.; Wahlgren, J.; Watson, D. C.; Wauben, M. H.; Weaver, A.; Webber, J. P.; Weber, V.; Wehman, A. M.; Weiss, D. J.; Welsh, J. A.; Wendt, S.; Wheelock, A. M.; Wiener, Z.; Witte, L.; Wolfram, J.; Xagorari, A.; Xander, P.; Xu, J.; Yan, X.; Yanez-Mo, M.; Yin, H.; Yuana, Y.; Zappulli, V.; Zarubova, J.; Zekas, V.; Zhang, J. Y.; Zhao, Z.; Zheng, L.; Zheutlin, A. R.; Zickler, A. M.; Zimmermann, P.; Zivkovic, A. M.; Zocco, D.; Zuba-Surma, E. K. Minimal information for studies of extracellular vesicles 2018 (MISEV2018): a position statement of the International Society for Extracellular Vesicles and update of the MISEV2014 guidelines. *J. Extracell. Vesicles* **2018**, *7*, 1535750.

(41) Trajkovic, K.; Hsu, C.; Chiantia, S.; Rajendran, L.; Wenzel, D.; Wieland, F.; Schwille, P.; Brügger, B.; Simons, M. Ceramide triggers budding of exosome vesicles into multivesicular endosomes. *Science* **2008**, *319*, 1244−1247.

(42) Bianco, F.; Perrotta, C.; Novellino, L.; Francolini, M.; Riganti, L.; Menna, E.; Saglietti, L.; Schuchman, E. H.; Furlan, R.; Clementi, E.; Matteoli, M.; Verderio, C. Acid sphingomyelinase activity triggers microparticle release from glial cells. *EMBO J.* **2009**, *28*, 1043−1054.

(43) Serban, K. A.; Rezania, S.; Petrusca, D. N.; Poirier, C.; Cao, D.; Justice, M. J.; Patel, M.; Tsvetkova, I.; Kamocki, K.; Mikosz, A.;

Schweitzer, K. S.; Jacobson, S.; Cardoso, A.; Carlesso, N.; Hubbard, W. C.; Kechris, K.; Dragnea, B.; Berdyshev, E. V.; McClintock, J.; Petrache, I. Structural and functional characterization of endothelial microparticles released by cigarette smoke. *Sci. Rep.* **2016**, *6*, 31596.

(44) del Conde, I.; Shrimpton, C. N.; Thiagarajan, P.; López, J. A. Tissue-factor-bearing microvesicles arise from lipid rafts and fuse with activated platelets to initiate coagulation. *Blood* **2005**, *106*, 1604–1611.

(45) Stoeger, V.; Liszt, K. I.; Lieder, B.; Wendelin, M.; Zopun, M.; Hans, J.; Ley, J. P.; Krammer, G. E.; Somoza, V. Identification of Bitter-Taste Intensity and Molecular Weight as Amino Acid Determinants for the Stimulating Mechanisms of Gastric Acid Secretion in Human Parietal Cells in Culture. *J. Agric. Food Chem.* **2018**, *66*, 6762–6771.

(46) Liszt, K. I.; Hans, J.; Ley, J. P.; Köck, E.; Somoza, V. Characterization of Bitter Compounds via Modulation of Proton Secretion in Human Gastric Parietal Cells in Culture. *J. Agric. Food Chem.* **2018**, *66*, 2295–2300.

(47) Kosaka, N.; Iguchi, H.; Yoshioka, Y.; Takeshita, F.; Matsuki, Y.; Ochiya, T. Secretory mechanisms and intercellular transfer of microRNAs in living cells. *J. Biol. Chem.* **2010**, *285*, 17442–17452.

(48) Yuyama, K.; Sun, H.; Mitsutake, S.; Igarashi, Y. Sphingolipid-modulated Exosome Secretion Promotes Clearance of Amyloid-β by Microglia. *J. Biol. Chem.* **2012**, *287*, 10977–10989.

(49) Dinkins, M. B.; Dasgupta, S.; Wang, G.; Zhu, G.; Bieberich, E. Exosome reduction in vivo is associated with lower amyloid plaque load in the 5XFAD mouse model of Alzheimer's disease. *Neurobiol. Aging* **2014**, *35*, 1792–1800.

(50) Qu, J. L.; Qu, X. J.; Zhao, M. F.; Teng, Y. E.; Zhang, Y.; Hou, K. Z.; Jiang, Y. H.; Yang, X. H.; Liu, Y. P. Gastric cancer exosomes promote tumour cell proliferation through PI3K/Akt and MAPK/ERK activation. *Dig. Liver Dis.* **2009**, *41*, 875–880.

(51) Ren, J.; Zhou, Q.; Li, H.; Li, J.; Pang, L.; Su, L.; Gu, Q.; Zhu, Z.; Liu, B. Characterization of exosomal RNAs derived from human gastric cancer cells by deep sequencing. *Tumor. Biol.* **2017**, *39*, 1010428317695012.

(52) Shelke, G. V.; Lässer, C.; Gho, Y. S.; Lötvall, J. Importance of exosome depletion protocols to eliminate functional and RNA-containing extracellular vesicles from fetal bovine serum. *J. Extracell. Vesicles* **2014**, *3*, 24783.

(53) Lehrich, B. M.; Liang, Y.; Khosravi, P.; Federoff, H.; Fiandaca, M. Fetal Bovine Serum-Derived Extracellular Vesicles Persist within Vesicle-Depleted Culture Media. *Int. J. Mol. Sci.* **2018**, *19*, 3538.

(54) Muratori, C.; Cavallin, L. E.; Krätzel, K.; Tinari, A.; De Milito, A.; Fais, S.; D'Aloja, P.; Federico, M.; Vullo, V.; Fomina, A.; Mesri, E. A.; Superti, F.; Baur, A. S. Massive secretion by T cells is caused by HIV Nef in infected cells and by Nef transfer to bystander cells. *Cell Host Microbe* **2009**, *6*, 218–230.

(55) Xiao, Z.; Blonder, J.; Zhou, M.; Veenstra, T. D. Proteomic analysis of extracellular matrix and vesicles. *J. Proteomics* **2009**, *72*, 34–45.

(56) Ma, L.; Li, Y.; Peng, J.; Wu, D.; Zhao, X.; Cui, Y.; Chen, L.; Yan, X.; Du, Y.; Yu, L. Discovery of the migrasome, an organelle mediating release of cytoplasmic contents during cell migration. *Cell Res.* **2015**, *25*, 24–38.

(57) Fertig, E. T.; Gherghiceanu, M.; Popescu, L. M. Extracellular vesicles release by cardiac telocytes: electron microscopy and electron tomography. *J. Cell Mol. Med.* **2014**, *18*, 1938–1943.

(58) Junquera, C.; Castiella, T.; Muñoz, G.; Fernández-Pacheco, R.; Luesma, M. J.; Monzón, M. Biogenesis of a new type of extracellular vesicles in gastrointestinal stromal tumors: ultrastructural profiles of spheresomes. *Histochem. Cell Biol.* **2016**, *146*, 557–567.

(59) Valcz, G.; Buzás, E. I.; Kittel, Á.; Krenacs, T.; Visnovitz, T.; Spisák, S.; Török, G.; Homolya, L.; Zsigrai, S.; Kiszler, G.; Antalffy, G.; Pálóczi, K.; Szállási, Z.; Szabó, V.; Sebestyén, A.; Solymosi, N.; Kalmár, A.; Dede, K.; Lőrincz, P.; Tulassay, Z.; Igaz, P.; Molnár, B. *En bloc* release of MVB-like small extracellular vesicle clusters by colorectal carcinoma cells. *J. Extracell. Vesicles* **2019**, *8*, 1596668.

(60) Forte, J. G.; Forte, T. M.; Machen, T. E. Histamine-stimulated hydrogen ion secretion by in vitro piglet gastric mucosa. *J. Physiol.* **1975**, *244*, 15–31.

(61) Forte, T. M.; Machen, T. E.; Forte, J. G. Ultrastructural and physiological changes in piglet oxyntic cells during histamine stimulation and metabolic inhibition. *Gastroenterology* **1975**, *69*, 1208–1222.

(62) Fellenius, E.; Elander, B.; Wallmark, B.; Haglund, U.; Helander, H. F.; Olbe, L. A micro-method for the study of acid secretory function in isolated human oxyntic glands from gastroscopic biopsies. *Clin. Sci.* **1983**, *64*, 423–431.

(63) Laboisse, C. L.; Augeron, C.; Couturier-Turpin, M. H.; Gespach, C.; Cheret, A. M.; Potet, F. Characterization of a newly established human gastric cancer cell line HGT-1 bearing histamine H2-receptors. *Cancer Res.* **1982**, *42*, 1541–1548.

(64) Sandle, G. I.; Fraser, G.; Fogg, K.; Warhurst, G. Properties of a potassium channel in cultured human gastric cells (HGT-1) possessing specific omeprazole binding sites. *Gut* **1993**, *34*, 1331–1338.

(65) Liszt, K. I.; Ley, J. P.; Rohm, B.; Stöger, V.; Köck, E.; Stuebler, A.; Hochkogler, C. M.; Somoza, M. M.; Widder, S.; Hans, J.; Somoza, V. Caffeine-induced activation of oral and gastric bitter taste receptors regulates gastric acid secretion. *Chem. Senses* **2015**, *40*, 602–603.

(66) González, D. A.; Barbieri van Haaster, M. M.; Quinteros Villarruel, E.; Brandt, M.; Benítez, M. B.; Stranieri, G. M.; Orman, B. Histamine stimulates secretion of extracellular vesicles with nucleotidase activity in rat submandibular gland. *Arch. Oral Biol.* **2018**, *85*, 201–206.

(67) Witwer, K. W.; Buzás, E. I.; Bemis, L. T.; Bora, A.; Lässer, C.; Lötvall, J.; Nolte-'t Hoen, E. N.; Piper, M. G.; Sivaraman, S.; Skog, J.; Thery, C.; Wauben, M. H.; Hochberg, F. Standardization of sample collection, isolation and analysis methods in extracellular vesicle research. *J. Extracell. Vesicles* **2013**, *2*, 20360.

(68) Prost, A.; Emami, S.; Gespach, C. Desensitization by histamine of H2 receptor-mediated adenylate cyclase activation in the human gastric cancer cell line HGT-1. *FEBS Lett.* **1984**, *177*, 227–230.

(69) Böing, A. N.; van der Pol, E.; Grootemaat, A. E.; Coumans, F. A. W.; Sturk, A.; Nieuwland, R. Single-step isolation of extracellular vesicles by size-exclusion chromatography. *J. Extracell. Vesicles* **2014**, *3*, 23430.

(70) Gardner, J. D.; Ciociola, A. A.; Robinson, M. Measurement of meal-stimulated gastric acid secretion by in vivo gastric autotitration. *J. Appl. Physiol.* **2002**, *92*, 427–434.

(71) Brisson, A. R.; Tan, S.; Linares, R.; Gounou, C.; Arraud, N. Extracellular vesicles from activated platelets: a semiquantitative cryo-electron microscopy and immuno-gold labeling study. *Platelets* **2017**, *28*, 263–271.

(72) Liszt, K. I.; Eder, R.; Wendelin, S.; Somoza, V. Identification of Catechin, Syringic Acid, and Procyanidin B2 in Wine as Stimulants of Gastric Acid Secretion. *J. Agric. Food Chem.* **2015**, *63*, 7775–7783.

(73) Riedel, A.; Pignitter, M.; Hochkogler, C. M.; Rohm, B.; Walker, J.; Bytof, G.; Lantz, I.; Somoza, V. Caffeine dose-dependently induces thermogenesis but restores ATP in HepG2 cells in culture. *Food Funct.* **2012**, *3*, 955–964.

(74) Stoeger, V.; Holik, A. K.; Hölz, K.; Dingjan, T.; Hans, J.; Ley, J. P.; Krammer, G. E.; Niv, M. Y.; Somoza, M. M.; Somoza, V. Bitter-Tasting Amino Acids l-Arginine and l-Isoleucine Differentially Regulate Proton Secretion via T2R1 Signaling in Human Parietal Cells in Culture. *J. Agric. Food Chem.* **2020**, *68*, 3434–3444.

(75) Mastronarde, D. N. Automated electron microscope tomography using robust prediction of specimen movements. *J. Struct. Biol.* **2005**, *152*, 36–51.

(76) Kuipers, J.; Giepmans, B. N. G. Neodymium as an alternative contrast for uranium in electron microscopy. *Histochem. Cell Biol.* **2020**, *153*, 271–277.